Radiology

Articular Cartilage of the Knee: Evaluation with Fluctuating Equilibrium MR Imaging—Initial Experience in Healthy Volunteers[1]

Garry E. Gold, MD
Brian A. Hargreaves, PhD
Shreyas S. Vasanawala, MD, PhD
Joshua D. Webb, MS
Ann S. Shimakawa, MS
Jean H. Brittain, PhD
Christopher F. Beaulieu, MD, PhD

Institutional review board approval and informed consent were obtained for this HIPAA-compliant study, whose purpose was to prospectively compare three magnetic resonance (MR) imaging techniques—fluctuating equilibrium, three-dimensional (3D) spoiled gradient-recalled acquisition in the steady state (SPGR), and two-dimensional (2D) fast spin echo (SE)—for evaluating articular cartilage in the knee. The study cohort consisted of 10 healthy volunteers (four men, six women; age range, 26–42 years). Cartilage signal-to-noise ratio (SNR), SNR efficiency, cartilage-fluid contrast-to-noise ratio (CNR), CNR efficiency, image quality, cartilage visibility, and fat suppression were compared. Cartilage volume was compared for the fluctuating equilibrium and 3D SPGR techniques. Compared with 3D SPGR and 2D fast SE, fluctuating equilibrium yielded the highest cartilage SNR efficiency and cartilage-fluid CNR efficiency ($P < .01$ for both). Image quality was similar with all sequences. Fluctuating equilibrium imaging yielded higher cartilage visibility than did 2D fast SE imaging ($P <. 01$) but worse fat suppression than did 3D SPGR and 2D fast SE imaging ($P < .04$). Cartilage volume measurements with fluctuating equilibrium and 3D SPGR were similar. Fluctuating equilibrium MR imaging is a promising method for evaluating articular cartilage in the knee.

[1] From the Departments of Radiology (G.E.G., S.S.V., C.F.B.), Electrical Engineering (B.A.H.), and Mechanical Engineering (J.D.W.), Stanford University, 300 Pasteur Dr, SO-68B, Stanford, CA 94305-5105; and GE Applied Sciences West Laboratory, Menlo Park, Calif (A.S.S., J.H.B.). Received December 23, 2004; revision requested February 23, 2005; revision received March 21; final version accepted April 15. Supported by NIH grant EB002524-01 and the Whitaker Foundation.

Osteoarthritis is extremely prevalent in society, occurring in more than one-third of people older than 35 years of age and in approximately 75% of people older than 75 years of age (1). In fact, osteoarthritis ranks second only to cardiovascular disease as a cause of chronic disability (1). The effects of osteoarthritis manifest as subchondral sclerosis and cysts, osteophytosis, and joint space narrowing as the result of degeneration and/or thinning of articular cartilage. Magnetic resonance (MR) imaging techniques may be important in studying the pathogenesis and evolution of osteoarthritis.

For accurately and reproducibly measuring cartilage volume, a technique that preserves cartilage signal is important to allow segmentation. In the identification of focal chondral defects, a technique with which the cartilage is relatively dark and fluid is bright makes it easy to identify surface defects. A technique that makes fluid relatively bright while cartilage signal is preserved may be useful for identifying chondral defects and in cartilage segmentation.

Considerable work in osteoarthritis has been devoted to imaging patients by using high-spatial-resolution three-dimensional (3D) MR imaging techniques. Three-dimensional spoiled gradient-recalled acquisition in the steady state (SPGR) MR imaging has been shown to enable high accuracy in the detection of cartilage lesions (2–4). The main disadvantages of 3D SPGR MR imaging are long imaging times (5–10 minutes) and the fact that the signal intensity of cartilage is higher than the signal intensity of fluid, which may make detection of surface lesions more difficult. In addition, 3D SPGR MR imaging involves the use of radiofrequency spoiling at the end of each repetition time to achieve near T1 weighting, resulting in a lower overall signal intensity and a lower signal-to-noise ratio (SNR) efficiency compared with those achieved with gradient-refocused techniques.

Recent work has produced several techniques that hold promise for improved evaluation of cartilage. Morphologic techniques include two-dimensional (2D) intermediate-weighted fast spin echo (SE) (5), short echo time projection reconstruction (6,7), and driven-equilibrium Fourier transform (8). A newer 3D gradient-echo technique that provides bright synovial fluid is 3D dual-echo steady-state imaging (9). More physiologic information can be obtained by using T2 mapping (10), gadolinium chelates to help map the proteoglycan content of articular cartilage (11), and sodium MR imaging (12).

Fluctuating equilibrium MR imaging is a variant of steady-state free precession (SSFP) that may be useful in imaging cartilage in the knee (13). Fluctuating equilibrium MR imaging may be particularly useful for detecting cartilage defects (14). Previous work with fluctuating equilibrium MR imaging has been limited by low spatial resolution, but improvements in automated shimming routines and gradient technology have allowed its use for volume and thickness measurements at a resolution comparable with that of 3D SPGR (15).

In fluctuating equilibrium MR, all magnetization is refocused over a repetition interval, but the radiofrequency phase cycles between 0° and 90°. The center frequency is set between water and fat, which are 220 Hz apart at 1.5 T, so the signal on successive excitations is alternately generated by fat and water protons. Each phase-encoding step is repeated twice, and data are parsed to form fat and water images. The lipid and water images are produced in the same imaging time.

The contrast produced by SSFP sequences, including fluctuating equilibrium MR, is also favorable for cartilage imaging. Like driven-equilibrium Fourier transform and 3D dual-echo steady-state MR imaging, fluctuating equilibrium MR imaging produces contrast based on the ratio of T1 to T2 in tissues. This results in bright signal from fluid while cartilage signal is preserved. Other SSFP approaches that may provide more reliable fat suppression at high spatial resolution are linear combination SSFP (16), Dixon imaging (17), and intermittent fat-saturated SSFP (18). Our current study examines the use of fluctuating equilibrium MR for imaging articular cartilage in 10 volunteers by using 3D SPGR and 2D fast SE MR imaging for comparison. We compared SNR and contrast-to-noise ratio (CNR) results, as well as image quality, cartilage visibility, and fat and water separation or fat suppression uniformity. We also compared the two 3D sequences for their ability to enable measurement of cartilage volumes in the knee.

Materials and Methods

The authors who are not employees of GE Healthcare had control of inclusion of any data and information that might present a conflict of interest for those authors who are employees of GE Healthcare.

Volunteers and Imaging

After approval of the institutional review board and informed consent were obtained, and in compliance with the Health Insurance Portability and Accountability Act, MR imaging was performed in 10 healthy volunteers. The right knees of the 10 volunteers (four men and six women), who ranged in age between 26 and 42 years, were imaged.

Published online
10.1148/radiol.2381042183

Radiology 2006; 238:712–718

Abbreviations:
CNR = contrast-to-noise ratio
SE = spin echo
SNR = signal-to-noise ratio
SPGR = spoiled gradient-recalled acquisition in the steady state
SSFP = steady-state free precession
3D = three-dimensional
2D = two-dimensional

Author contributions:
Guarantor of integrity of entire study, G.E.G.; study concepts/study design or data acquisition or data analysis/interpretation, all authors; manuscript drafting or manuscript revision for important intellectual content, all authors; approval of final version of submitted manuscript, all authors; literature research, G.E.G.; clinical studies, G.E.G., S.S.V., J.D.W., J.H.B., C.F.B.; experimental studies, all authors; statistical analysis, G.E.G., J.D.W.; and manuscript editing, G.E.G., B.A.H., C.F.B.

Address correspondence to G.E.G.
(e-mail: *gold@stanford.edu*).

See Materials and Methods for pertinent disclosures.

Volunteers had no history of knee pain or surgery in either knee. The right knees were imaged for ease of positioning in the MR imaging unit. All images were acquired with a 1.5-T MR imaging unit (Signa Twinspeed; GE Healthcare, Milwaukee, Wis) with high-performance gradients (maximum gradient strength, 40 mT/m; maximum slew rate, 150 [mT · m^{-1}]/sec) by using a transmit-receive quadrature knee coil. Automated higher-order shimming preceded all acquisitions (19). Acquisition resolution was kept constant among all imaging sequences, with a matrix of 512 × 256, 2-mm-thick sections, frequency encoding in the superoinferior direction, and a 16-cm field of view.

Fluctuating equilibrium MR images were acquired with a repetition time msec/echo time msec of 6.6/1.8 and a flip angle of 25°. Forty-four sections were obtained with one signal acquired and were reconstructed with zero-padding interpolation at 1-mm intervals. A partial echo was used to reduce the repetition time. The imaging bandwidth was ±62.5 kHz, and the imaging time was 2 minutes 43 seconds. Two-dimensional fast SE images were acquired with 5000/41, two acquisitions (interleaved 2-mm-thick sections with no gap), an echo train length of eight, and fat suppression. The imaging bandwidth was ±16 kHz, and the imaging time was 5 minutes 30 seconds. Three-dimensional SPGR images were acquired with 40/7, a flip angle of 40°, and fat suppression. Forty-four sections were obtained with one signal acquired and reconstructed with zero-padding interpolation at 1-mm intervals. The imaging bandwidth was ±31.25 kHz, and the imaging time was 8 minutes 56 seconds. Images were acquired in the sagittal plane so that we could evaluate the articular cartilage of the femur and tibia in the medial and lateral joint compartments, as well as the articular cartilage in the medial and lateral patellofemoral compartments.

Imaging of Phantom

A cartilage phantom (20) was also imaged with the same parameters used for imaging the volunteers. The phantom consisted of a spherical portion in contact with a flat portion. Each portion was coated with urethane gelatin (Urethane RTV System; Tap Plastics, Dublin, Calif) and doped with water so that the relaxation times in the phantom would mimic those in cartilage. Fluid containing manganese chloride (Sigma Chemical, St Louis, Mo) was used to simulate synovial fluid. After imaging, the phantom was taken apart and the volumes of the urethane gelatin on the spherical and flat portions were determined through water displacement testing in a graduated cylinder; this testing was repeated three times.

Image Evaluation

Signal in cartilage, signal in synovial fluid, and noise, respectively, were measured in all volunteers in three regions of interest placed in the trochlear cartilage, patellofemoral joint fluid, and artifact-free areas of noise. Measurements were performed by a single radiologist (G.E.G.) with 10 years of experience in interpreting MR images of the knee. The circular region of interest for cartilage and fluid signal measurements was 3 mm in diameter. The circular region of interest for noise measurements was 9 mm in diameter. The SNR and SNR efficiency (SNR divided by the square root of the imaging time) for cartilage were calculated. The fluid-cartilage CNR and the fluid-cartilage CNR efficiency (CNR divided by the square root of the imaging time) were calculated.

Three experienced radiologists (G.E.G., S.S.V., and C.F.B.) with 10, 4, and 15 years of experience, respectively, in interpreting MR images of the knee graded all of the images. Image quality was graded on a scale from 0 to 3 as follows: A score of 0 indicated high image noise with artifacts; a score of 1, high image noise with minor artifacts; a score of 2, high image noise and no artifacts; and a score of 3, low image noise and no artifacts. Cartilage visibility was graded on a scale from 0 to 3 as follows: A score of 0 indicated that cartilage was not visible; a score of 1, that cartilage was somewhat distinct from subchondral bone but dark; a score of 2, that cartilage was visible but its deep layers and surface were indistinct; and a score of 3, that cartilage was bright and its entire thickness was visible. Uniformity of fat suppression or fat and water separation was graded on a scale from 0 to 3 as follows: A score of 0 indicated water suppression; a score of 1, that fat near cartilage was not suppressed; a score of 2, that there was patchy failure of fat suppression not near cartilage; and a score of 3, that there was near-perfect fat suppression.

Cartilage volume was compared between 3D SPGR and fluctuating equilibrium MR images. A custom semiautomated software package (Bodybuilder; Vicon Motion Systems, Lake Forest, Calif) was used to segment the articular cartilage and measure the volumes. In the phantom, cartilage (urethane) was segmented three times for both sequences; the resulting values were compared with the measured volume. In the volunteers, cartilage volumes for the tibia, femur, and patella were compared between the two sequences. One observer (J.D.W.) with 2 years of experience in image segmentation performed segmentation of the cartilage while being supervised by a more experienced observer (G.E.G.). So that we could evaluate intraobserver variability, one observer (J.D.W.) resegmented the femoral cartilage with both the fluctuating equilibrium and the 3D SPGR sequences three times by using a single volunteer data set.

Statistical Analysis

Statistical analysis was performed by using two computer programs (Excel, version 11.1.1, Microsoft, Redmond, Wash; and SPSS, version 11.0, SPSS, Chicago, Ill). The three imaging sequences were pairwise compared with respect to SNR, SNR efficiency, CNR, and CNR efficiency by using a paired-sample *t* test. The mean scores assigned by the three radiologists for the three imaging sequences were also pairwise compared with respect to image quality, cartilage visibility, and uniformity of fat suppression or fat and water separation by using a Wilcoxon signed rank test. The two 3D sequences were pairwise compared with respect to cartilage vol-

umes measured in three bones (the patella, femur, and tibia) by using a paired *t* test. A *P* value of less than .05 was considered to indicate significance for the paired *t* tests and the Wilcoxon signed rank test. The coefficient of variation was calculated for intraobserver variability in femoral cartilage volume segmentation with the fluctuating equilibrium and 3D SPGR sequences.

Figure 1

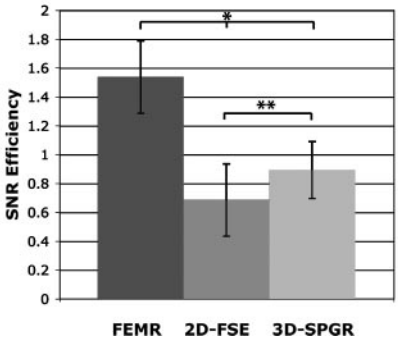

Figure 1: Bar graph shows cartilage SNR efficiency values for fluctuating equilibrium *(FEMR)*, 2D fast SE, and 3D SPGR MR imaging sequences. SNR efficiency is SNR divided by the square root of the imaging time. The cartilage SNR efficiency was significantly higher for the fluctuating equilibrium sequence (* = $P < .01$) than for both the 3D SPGR and the 2D fast SE sequences. The cartilage SNR efficiency for the 3D SPGR sequence was significantly higher than that for the 2D fast SE sequence (** = $P < .01$). Error bars indicate standard deviations.

Figure 2

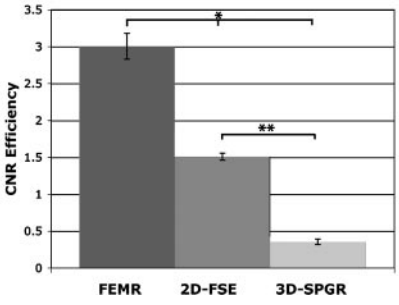

Figure 2: Bar graph shows cartilage-fluid CNR efficiency values for fluctuating equilibrium *(FEMR)*, 2D fast SE, and 3D SPGR MR imaging sequences. The cartilage-fluid CNR efficiency was significantly higher for the fluctuating equilibrium sequence than for either the 3D SPGR or the 2D fast SE sequence (* = $P < .01$). The cartilage-fluid CNR efficiency for the 2D fast SE sequence was significantly higher than that for the 3D SPGR sequence (** = $P < .01$). Error bars indicate standard deviations.

Results

Mean cartilage SNR was statistically equivalent on the 3D fluctuating equilibrium (20.1 ± 4 [standard deviation]) and the 3D SPGR (21.3 ± 2) MR images but was significantly higher on these two types of images than on the 2D fast SE images (12 ± 3, $P < .02$). Mean cartilage SNR efficiency was significantly higher with fluctuating equilibrium imaging (1.5 ± 0.25) than with either 3D SPGR (0.9 ± 0.20) or 2D fast SE (0.7 ± 0.20, $P < .01$) imaging (Fig 1). Mean cartilage SNR efficiency was also significantly higher with 3D SPGR than with 2D fast SE imaging ($P < .01$), probably because of the longer echo time in 2D fast SE imaging.

Mean fluid-cartilage CNR was higher with the fluctuating equilibrium sequence (38.3 ± 7.6) than with either the 2D fast SE (27.4 ± 9.8) or the 3D SPGR (8.2 ± 0.86, $P < .01$) sequence. Mean fluid-cartilage CNR efficiency was much higher with fluctuating equilibrium (3.0 ± 0.17) than with 2D fast SE (1.5 ± 0.05) and 3D SPGR imaging (0.4 ± 0.04, $P < .01$) (Fig 2). Mean fluid-cartilage CNR efficiency was also higher with 2D fast SE than with 3D SPGR imaging ($P < .01$). High cartilage and fluid signal intensity were seen on the fluctuating equilibrium water MR images (Fig 3).

Mean image quality was between good and excellent for the fluctuating equilibrium (ie, 2.3), 3D SPGR (2.5), and 2D fast SE (2.7) sequences; there was no significant difference between these values. Banding artifacts were seen in the edges of fluctuating equilibrium MR images and slightly lowered the image quality scores. Cartilage visibility was graded as excellent for both the fluctuating equilibrium (2.8) and the 3D SPGR (3.0) sequences; the grades for both sequences were significantly higher than the grade for the 2D fast SE sequence (2.0, $P < .01$). However, mean fat suppression or fat and water separation uniformity scores for 2D fast SE (2.8) and 3D SPGR (2.8) imaging were significantly better than the score for fluctuating equilibrium imaging (2.0, $P < .04$). Fluid was easily distinguished from cartilage on fluctuating equilibrium and 2D fast SE images but not on 3D SPGR images (Fig 4).

As compared with the graduated

Figure 3

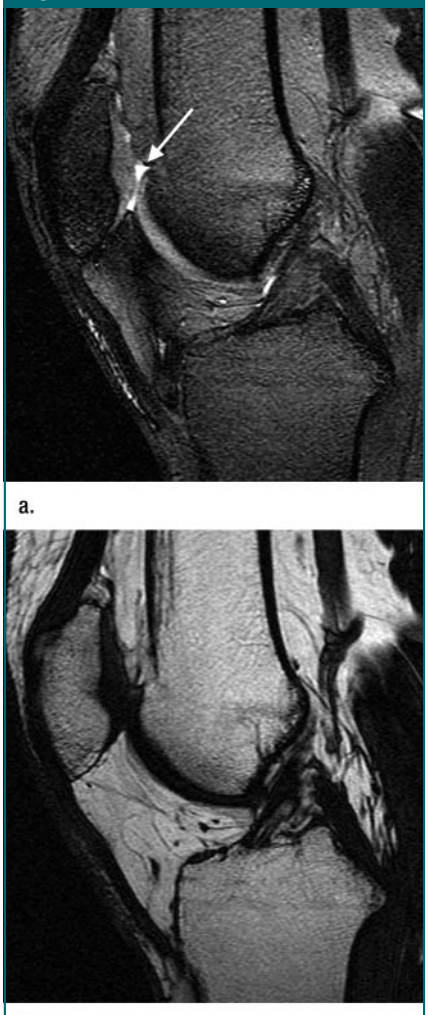

Figure 3: **(a)** Sagittal fluctuating equilibrium MR water image (6.6/1.8; flip angle, 25°) and **(b)** lipid image (6.6/1.8; flip angle, 25°) in healthy 29-year-old female volunteer. The signal intensity of fluid (arrow) is high compared with the signal intensity of the articular cartilage.

cylinder displacement test results, cartilage volume results with the two 3D sequences (fluctuating equilibrium and SPGR) in the phantom showed high accuracy (Fig 5a). Both sequences enabled measurement of volumes in the phantom to within the error of the displacement test. In all 10 of our volunteers, similar measurements of volumes with fluctuating equilibrium and 3D SPGR imaging were seen (Fig 5b). Paired *t* test results indicated that the cartilage volumes measured in the patella, femur, and tibia in the volunteers were not statistically different between fluctuating equilibrium and 3D SPGR imaging ($P > .5$). Fluctuating equilibrium MR imaging enabled accurate segmentation of the cartilage volumes in the femur, patella, and tibia (Fig 6). The coefficient of variation for intraobserver variability for our observer who segmented the femoral cartilage volumes with fluctuating equilibrium MR images was 1.2%, while with 3D SPGR MR images, it was 1.3%.

Discussion

Fluctuating equilibrium MR imaging provides excellent contrast between synovial fluid and cartilage while preserving signal from the cartilage itself. The contrast seen with fluctuating equilibrium MR imaging is based on the ratio of T1 to T2 and is similar to that seen with driven-equilibrium Fourier transform in previous studies (8). Other methods of fat suppression or fat and water separation that may be combined with SSFP include Dixon imaging (17), phase-sensitive reconstruction (21), intermittent fat suppression (18), and linear combinations of SSFP (16). All of these SSFP-based techniques can result in banding artifacts at long repetition times or in the presence of main field inhomogeneity (22).

The use of fat suppression or fat and water separation in cartilage imaging is important for improving the dynamic range of signal in the cartilage and reducing chemical shift artifacts. In the present study, fat and water separation with fluctuating equilibrium MR was not as uniform as fat suppression with 2D fast SE or 3D SPGR, but it was sufficient to provide good contrast for cartilage imaging. Banding artifacts were seen at the edges of the fluctuating equilibrium MR images, and these artifacts reduced the quality scores for these images but did not interfere with cartilage volume measurements. Localized shimming may be helpful in reducing banding artifacts (19).

Our study had several limitations. Only one observer measured cartilage volumes, so interobserver variability was not assessed. Although we were able to confirm the absolute accuracy of our cartilage volume measurements in the phantom, we could not do so for the cartilage volume measurements in our volunteers. We included healthy volunteers rather than patients with osteoarthritis, in whom segmentation could be more difficult. Overall, however, fluctuating equilibrium MR imaging proved to be a rapid and promising method for assessing cartilage volumes.

Fluctuating equilibrium MR imaging may be useful in volume and thickness measurements. Three-dimensional SPGR MR imaging is commonly used for cartilage volume and thickness measurements but is time consuming and does not provide bright fluid that outlines surface defects (23). Volume and thick-

Figure 4

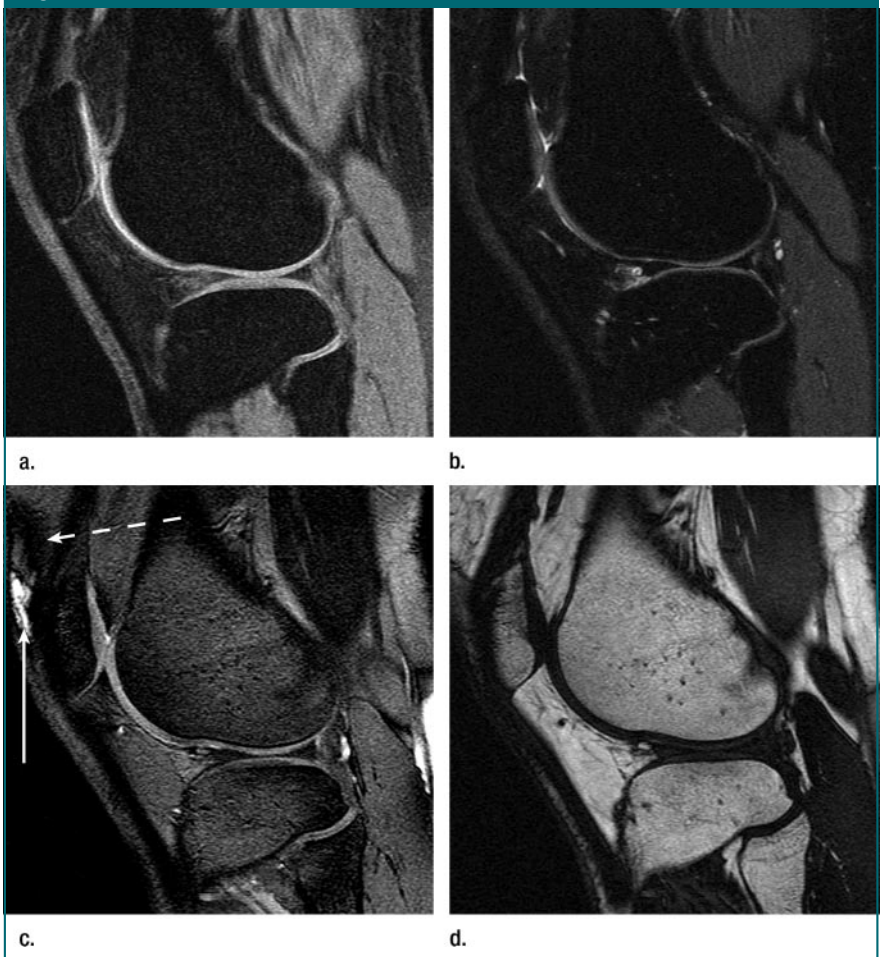

Figure 4: **(a)** Sagittal 3D SPGR (40/7; flip angle, 40°), **(b)** 2D fast SE (5000/41; echo train length, eight), **(c)** fluctuating equilibrium MR water (6.6/1.8; flip angle, 25°), and **(d)** fluctuating equilibrium MR lipid (6.6/1.8; flip angle, 25°) images in healthy 26-year-old female volunteer. An area of poor fat and water separation (solid arrow), as well as a banding artifact (dashed arrow), is seen near the patella on **c**.

Figure 5

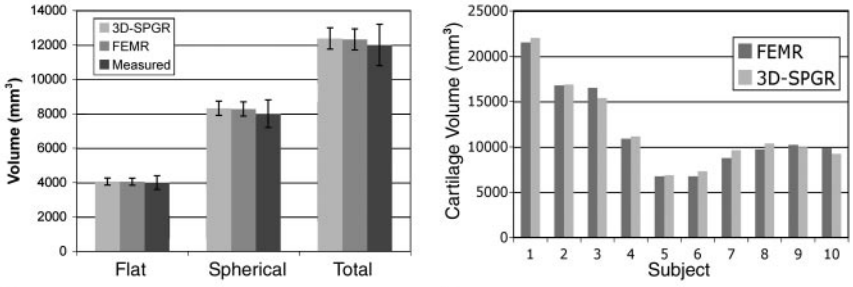

Figure 5: Bar graphs show comparison of cartilage volume measurements between fluctuating equilibrium *(FEMR)* and 3D SPGR MR imaging sequences. **(a)** Graph shows comparison between fluctuating equilibrium and 3D SPGR measurements and actual measured cartilage volume in the phantom. Error bars indicate standard deviations. **(b)** Graph shows comparison of cartilage volume as measured with each sequence in the femurs of 10 healthy volunteers. There were no significant differences between cartilage volumes measured with the fluctuating equilibrium sequence and those measured with the 3D SPGR sequence in the femur, tibia, and patella ($P > .5$, paired *t* test).

Figure 6

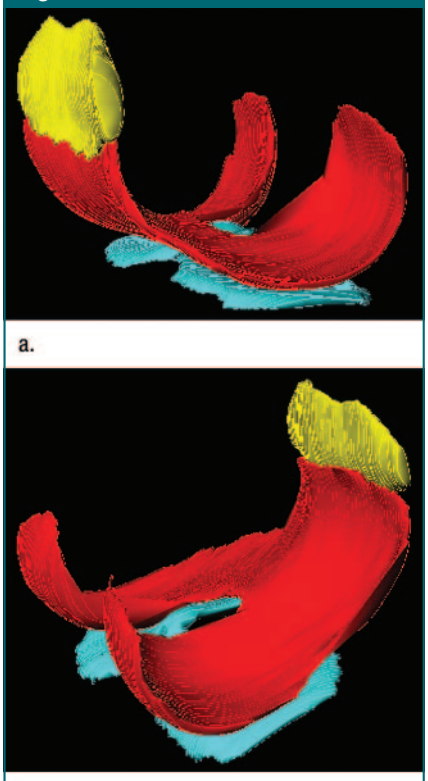

Figure 6: Example of cartilage segmentation performed by using fluctuating equilibrium MR imaging in healthy 32-year-old male volunteer. Cartilage surfaces on the femur (red), patella (yellow), and tibia (blue) are all well seen.

ness measurements obtained with a 3D technique may be useful in following up patients with osteoarthritis. Fluctuating equilibrium MR imaging has the potential to replace 3D SPGR MR imaging for quantifying thickness and volume in longitudinal studies.

Because with this technique the joint fluid remains bright, fluctuating equilibrium MR imaging may be more useful in the detection of cartilage surface defects than 3D SPGR MR imaging (24). Although joint fluid is bright in fluctuating equilibrium MR imaging, this technique may not be as useful as fast SE MR imaging for examining other joint structures. The use of fluctuating equilibrium MR imaging in the diagnosis of meniscal, tendon, or ligament disease will be the subject of future studies.

In conclusion, fluctuating equilibrium MR imaging seems to hold promise for the evaluation of articular cartilage. Better depiction of marrow edema, improved fat suppression, and artifact reduction are important in improving fluctuating equilibrium MR imaging. Studies that involve more subjects and entail evaluation of the ability of fluctuating equilibrium MR imaging to show cartilage lesions and to enable measurement of cartilage thickness and volumes in patients with osteoarthritis are important to validate this technique.

References

1. Felson DT, Lawrence RC, Dieppe PA, et al. Osteoarthritis: new insights. I. The disease and its risk factors. Ann Intern Med 2000; 133:635–646.
2. Disler DG. Fat-suppressed three-dimensional spoiled gradient-recalled MR imaging: assessment of articular and physeal hyaline cartilage. AJR Am J Roentgenol 1997;169: 1117–1123.
3. Recht MP, Piraino DW, Paletta GA, Schils JP, Belhobek GH. Accuracy of fat-suppressed three-dimensional spoiled gradient-echo FLASH MR imaging in the detection of patellofemoral articular cartilage abnormalities. Radiology 1996;198:209–212.
4. Wang SF, Cheng HC, Chang CY. Fat-suppressed three-dimensional fast spoiled gradient-recalled echo imaging: a modified FS 3D SPGR technique for assessment of patellofemoral joint chondromalacia. Clin Imaging 1999;23:177–180.
5. Potter HG, Linklater JM, Allen AA, Hannafin JA, Haas SB. Magnetic resonance imaging of articular cartilage in the knee: an evaluation with use of fast-spin-echo imaging. J Bone Joint Surg Am 1998;80:1276–1284.
6. Brossmann J, Frank LR, Pauly JM, et al. Short echo time projection reconstruction MR imaging of cartilage: comparison with fat-suppressed spoiled GRASS and magnetization transfer contrast MR imaging. Radiology 1997;203:501–507.
7. Gold GE, Thedens DR, Pauly JM, et al. MR imaging of articular cartilage of the knee: new methods using ultrashort TEs. AJR Am J Roentgenol 1998;170:1223–1226.
8. Hargreaves BA, Gold GE, Lang PK, et al. MR imaging of articular cartilage using driven equilibrium. Magn Reson Med 1999;42:695–703.
9. Hardy PA, Recht MP, Piraino D, Thomasson D. Optimization of a dual echo in the steady state (DESS) free-precession sequence for imaging cartilage. J Magn Reson Imaging 1996;6:329–335.
10. Mosher TJ, Dardzinski BJ, Smith MB. Human articular cartilage: influence of aging and early symptomatic degeneration on the spatial variation of T2—preliminary findings at 3 T. Radiology 2000;214:259–266.
11. Burstein D, Velyvis J, Scott KT, et al. Protocol issues for delayed Gd(DTPA)(2-)-enhanced MRI (dGEMRIC) for clinical evaluation of articular cartilage. Magn Reson Med 2001;45:36–41.
12. Reddy R, Insko EK, Noyszewski EA, Dandora R, Kneeland JB, Leigh JS. Sodium MRI

of human articular cartilage in vivo. Magn Reson Med 1998;39:697–701.

13. Vasanawala SS, Pauly JM, Nishimura DG. Fluctuating equilibrium MRI. Magn Reson Med 1999;42:876–883.

14. Vasnawala SS, Pauly JM, Nishimura DG, Gold GE. MR imaging of knee cartilage with FEMR. Skeletal Radiol 2002;31:574–580.

15. Eckstein F, Schnier M, Haubner M, et al. Accuracy of cartilage volume and thickness measurements with magnetic resonance imaging. Clin Orthop Relat Res 1998;352:137–148.

16. Vasanawala SS, Pauly JM, Nishimura DG. Linear combination steady-state free precession MRI. Magn Reson Med 2000;43:82–90.

17. Reeder SB, Pelc NJ, Alley MT, Gold GE. Rapid MR imaging of articular cartilage with steady-state free precession and multipoint fat-water separation. AJR Am J Roentgenol 2003;180:357–362.

18. Scheffler K, Heid O, Hennig J. Magnetization preparation during the steady state: fat-saturated 3D TrueFISP. Magn Reson Med 2001; 45:1075–1080.

19. Spielman DM, Adalsteinsson E, Lim KO. Quantitative assessment of improved homogeneity using higher-order shims for spectroscopic imaging of the brain. Magn Reson Med 1998;40:376–382.

20. Gold GE, Besier TF, Draper CE, Asakawa DS, Delp SL, Beaupre GS. Weight-bearing MRI of patellofemoral joint cartilage contact area. J Magn Reson Imaging 2004;20:526–530.

21. Hargreaves BA, Vasanawala SS, Nayak KS, Hu BS, Nishimura DG. Fat-suppressed steady-state free precession imaging using phase detection. Magn Reson Med 2003;50: 210–213.

22. Hargreaves BA, Gold GE, Beaulieu CF, Vasanawala SS, Nishimura DG, Pauly JM. Comparison of new sequences for high-resolution cartilage imaging. Magn Reson Med 2003;49:700–709.

23. Eckstein F, Westhoff J, Sittek H, et al. In vivo reproducibility of three-dimensional cartilage volume and thickness measurements with MR imaging. AJR Am J Roentgenol 1998;170:593–597.

24. Mosher TJ, Pruett SW. Magnetic resonance imaging of superficial cartilage lesions: role of contrast in lesion detection. J Magn Reson Imaging 1999;10:178–182.